IV International Conference on Particle-based Methods – Fundamentals and Applications
PARTICLES 2015
E. Oñate, M. Bischoff, D.R.J. Owen, P. Wriggers & T. Zohdi (Eds)

NUMERICAL STUDY OF FLUID-STRUCTURE INTERACTION WITH MACRO-SCALE PARTICLE METHODS

GUANGZHENG ZHOU

State Key Laboratory of Multiphase Complex Systems, Institute of Process Engineering,
Chinese Academy of Sciences, Beijing 100190, China
E-mail address: gzzhou@ipe.ac.cn

Key words: Fluid-structure interaction, Particle methods, Smoothed particle hydrodynamics, Macro-scale pseudo-particle modelling, Gas-solid suspension, Outflow.

Abstract The problems of fluid-structure interaction (FSI) are often encountered in different industries as well as the nature. The macro-scale particle methods are advantageous in the FSI simulations, which include smoothed particle hydrodynamics (SPH), macro-scale pseudo-particle modelling (MaPPM), and so forth. Compared with the grid-based numerical techniques, particle methods could provide the flow and/or deformation details without complex tracking of interfaces. The progress of FSI simulation of multiphase flows with rigid particles is presented, and some major findings about heterogeneous structures are stressed. Meanwhile, weakly compressible outflow from elastic tube is investigated, and some preliminary results of flow details are presented. The possible development of macro-scale particle methods in the FSI simulation is prospected finally.

1 INTRODUCTION

The problems of fluid-structure interaction (FSI) are extensively encountered in many industrial applications as well as biological systems, such as multi-phase flows in fluidized beds, transports in flexible pipeline, and coupled membrane-fluid systems. In general, they are often too complex to be solved analytically, while numerical simulation could play an important role in this aspect. The well-known arbitrary Lagrangian-Eulerian method[1] (ALE) formulates the fluid field on deforming grids, and takes into account the convection of these grid points. Nevertheless, the remeshing procedure in ALE is usually rather complicated and also computationally expensive, particularly for large deformation. On the other hand, the fluid domain of immersed boundary method[2] (IBM) is based on uniform background grids, and the immersed set of boundary points interact with the fluid through the introduction of body forces. Actually, the distributed Lagrange multiplier based fictitious domain method[3] (DLM\FDM) shares many similarities with IBM, but the force between the fluid and structure in DLM\FDM is distributed using an integral formulation. However, there still exists some difficulty in the accurate representation of structure with finite volume and/or complicated constitutive laws in the above two fixed grid methods as well as their variants.

In contrast, macro-scale particle methods offer notable advantages in FSI problems, including smoothed particle hydrodynamics[4,5] (SPH), macro-scale pseudo-particle modelling[6] (MaPPM), moving particle semi-implicit (MPS) method[7], and so forth. In these approaches, the continuum is discretized into a collection of particles without background

meshes, and these particles move in Lagrangian manner according to the macro-scale interaction with their neighboring ones. Consequently, the large deformation of material interface or free surface is naturally handled without the vexing problem of mesh distortion. Actually, the classical SPH method originally developed for astrophysical contexts, has been extended to various fields due to the conceptual simplicity[8,9], including turbulent flow, multiphase flows, non-Newtonian flows, and elastic dynamics.

In the FSI simulations with particle methods, complex tracking of interface is completely avoided. However, the structure/solid could be rigid or elastic, which corresponds to totally different treatment. As for the rigid solids usually in the form of a large number of particles, the interactions between particles are generally depicted by the discrete element method (DEM) [10,11]. DEM follows the motion of every particle, while their interactions are based on certain contact model. On the other hand, for the interaction between elastic structure and fluid, both of them could be simulated by unified SPH descriptions with their own constitutive relations. However, the classical SPH generally suffers from the problem of so-called "tensile instability" in the simulations of elastic or brittle solid[8]. When the SPH particles are under a tensile state, they tend to form small clumps, resulting in unphysical fractures eventually. The source of this instability has been analyzed in details by Swegle et al. [12], and several techniques have been proposed to remedy this drawback, such as adding extra stress points[13], corrective smoothed particle method[14] (CSPM), and artificial stress method [15,16]. In the artificial stress method, additional artificial stress was particularly incorporated into the momentum equation by mimicking atomic forces. The artificial stress exerted a small repulsive force for particles in the state of tensile stress, and thus effectively prevented them from clustering. Based on the analysis of the dispersion relation in elastic wave, the resulting algorithm of artificial stress was found to be effective and accurate for various benchmark problems in elastic dynamics[16,17].

A good understanding of FSI phenomena is crucial to relevant industrial applications. As for the FSI problem of rigid solids, the direct numerical simulation (DNS) of classical multi-phase suspensions is generally full of challenges due to its large computational cost. On the other hand, most simulations on FSI problems cope with the nearly incompressible fluid and hypoelastic structure[17-19], and thus further study of FSI problems with weakly compressible flow would be quite significant. In this paper, the progress of FSI simulation of rigid particles is presented, which combines MaPPM (or SPH) with DEM. Also, weakly compressible outflow from elastic tube is investigated with unified SPH formulations, where a particular outflow boundary is applied, and the artificial stress is employed to remove the tensile instability in elastic solid. Besides, the outflow simulation is based on the previous researches on selective withdrawal from rigid microcavity[20] and immiscible displacement in rigid cavity-fracture structures[21].

2 NUMERICAL FORMULATIONS OF FSI PROBLEMS

2.1 SIMULATION OF FLUIDS

In nature, the macro-scale particle methods are based on interpolation theory. An arbitrary field variable $f(\mathbf{r})$ at location $\mathbf{r}$ is evaluated as sum over a set of neighboring points (particles)

$$f(\mathbf{r}) = \sum_{j=1}^{N} \frac{m_j}{\rho_j} f(\mathbf{r}_j) W(\mathbf{r} - \mathbf{r}_j, h) \tag{1}$$

where m_j and ρ_j are the mass and density of particle j; while $W(\mathbf{r} - \mathbf{r}_j, h)$ is the weighting function with h as its smoothing length. The weighting function should satisfy several requirements, including the normalization condition and the property of Dirac delta function. Among a number of weighting functions, the cubic spline is employed for both fluid and solid in the present work[8].

Following Eq. 1, the local density of particle i is given by

$$\rho_i = \sum_j m_j W(|\mathbf{r}_i - \mathbf{r}_j|, h) \tag{2}$$

In regard to the SPH formulation of Navier-Stokes equation, there exist different forms of pressure component as well as viscous component. Based on the symmetric pressure which conserves linear and angular momentum exactly, the momentum equation of SPH particles could be written as[22]

$$\frac{d\mathbf{v}_i}{dt} = -\sum_j m_j \left(\frac{P_i}{\rho_i^2} + \frac{P_j}{\rho_j^2}\right) \nabla_i W_{ij} + \sum_j \frac{m_j (\mu_i + \mu_j)(\mathbf{v}_i - \mathbf{v}_j)}{\rho_i \rho_j} \left(\frac{1}{r_{ij}} \frac{\partial W_{ij}}{\partial r_i}\right) + \mathbf{g} \tag{3}$$

where $\mathbf{v}$ is the velocity, μ is the dynamic viscosity, and ∇_i denotes the gradient with respect to its coordinates.

Besides, the two-dimensional version of momentum equation in MaPPM[6] is

$$\frac{d\mathbf{v}_i}{dt} = -c_{\mathrm{f}}^2 \sum_j \frac{2}{\rho_i + \rho_j} \nabla_i W_{ij} + 4\mu \sum_j \frac{(\mathbf{v}_j - \mathbf{v}_i) W_{ij}}{0.25(\rho_i + \rho_j)(D_i + D_j)} + \mathbf{g} \tag{4}$$

$$D_i = \sum_j r_{ij}^2 W_{ij} \tag{5}$$

where c_{f} is numerical sound speed of fluid in the artificial state equation. The compressibility of fluid could be adjusted with suitable choice of numerical sound speed, and the incompressiblity is approximately guaranteed through sufficiently large sound speed.

2.2 SIMULATION OF EALSTIC STRUCTURES

The stress tensor σ of momentum conservation could be decomposed into the isotropic pressure P and the deviatoric stress S. In regard to elastic solid with Hooks' law, the Jaumann rate is commonly adopted to satisfy the material frame indifference of large deformation. The evolution of deviatoric stress in elastic solid[16,23] can be written as

$$\frac{dS^{\alpha\beta}}{dt} = 2G\left(\dot{\varepsilon}^{\alpha\beta} - \frac{1}{3}\delta^{\alpha\beta}\dot{\varepsilon}^{\alpha\beta}\right) + S^{\alpha\gamma}\Omega^{\beta\gamma} + \Omega^{\alpha\gamma}S^{\gamma\beta} \tag{6}$$

where G is the shear modulus, $\dot{\varepsilon}$ is the strain rate, Ω is the rotation tensor, while superscripts α and β indicate the spatial coordinates.

Moreover, the momentum equation of solid can be depicted by the following form

$$\frac{d\mathbf{v}_i^{\alpha}}{dt} = -\sum_j m_j \left(\frac{\sigma_i^{\alpha\beta}}{\rho_i^2} + \frac{\sigma_j^{\alpha\beta}}{\rho_j^2} + \Pi_{ij} + R_{ij}^{\alpha\beta} f^q\right)\nabla_i W_{ij} + \mathbf{g} \tag{7}$$

where Π_{ij} and $R_{ij}^{\alpha\beta} f^n$ refer to the terms of artificial viscosity and artificial stress[16], respectively.

Generally, the introduction of artificial viscosity could effectively enhance the stability of numerical algorithm. Among various types of artificial viscosity, a popular one[24] is

$$\Pi_{ij} = \begin{cases} \dfrac{-\alpha_\Pi c_s \mu_{ij} + \beta_\Pi \mu_{ij}^2}{\bar{\rho}_{ij}}, & \mathbf{v}_{ij}\cdot\mathbf{r}_{ij} < 0; \\ 0, & \mathbf{v}_{ij}\cdot\mathbf{r}_{ij} > 0 \end{cases} \tag{8}$$

where c_s represents the numerical speed of sound in the solid, $\mu_{ij} = \dfrac{h\mathbf{v}_{ij}\cdot\mathbf{r}_{ij}}{\mathbf{r}_{ij}^2 + 0.01h^2}$, and $\bar{\rho}_{ij} = \dfrac{\rho_i + \rho_j}{2}$. The linear term with α_Π produces shear and bulk viscosity, while the quadratic term with β_Π suppresses the unphysical penetration among particles.

In addition, the term of artificial stress has the expression[16]

$$R_{ij}^{\alpha\beta} f^q = (R_i^{\alpha\beta} + R_j^{\alpha\beta})\left(\frac{W(r_{ab})}{W(d)}\right)^q \tag{9}$$

where d is the initial interparticle distance, and q is a parameter. To obtain the artificial stress R, the original stress tensor is diagonalised for the signs of principal stresses, and the diagonal components of artificial stress in the rotated frame could be specified as follows

$$\bar{R}_i^{\alpha\alpha} = \begin{cases} -e\dfrac{\bar{\sigma}_i^{\alpha\alpha}}{\rho_i^2}, & \bar{\sigma}_i^{\alpha\alpha} > 0; \\ 0, & \bar{\sigma}_i^{\alpha\alpha} \le 0 \end{cases} \tag{10}$$

where e is also a parameter. The artificial stress in the original coordinates is further calculated through rotating the coordinates back. Besides, the strain rate $\dot{\varepsilon}$ and rotation tensor Ω in Eq. 6 are obtained with corresponding SPH formulations.

3 FSI SIMULATION OF MULTIPHASE FLOWS WITH RIGID PARTICLES

As for the gas-solid or liquid–solid multiphase flows in industrial systems, such as fluidized bed, the systems usually involve huge number of rigid particles. In the DNS simulation of such flows using SPH or MaPPM, the size of numerical parcticles should be much smaller than that of solid particles. Therefore, the computational cost is generally in proportional to the involved particle number of the system. Potapov et al.[25] carried out the investigation of liquid–solid flows combining SPH and DEM with soft-particle technique. In the shear-cell simulation, there were only 8 or 17 solid particles, corresponding to solid area fractions of 17% and 37%, respectively.

Furthermore, the simulation of gas-solid suspension with 1024 particles was implemented by couping MaPPM and DEM with hard-sphere collisions[26], based on the large-scale parallel

computating with CPU (central processing unit) clusters. The parallel was realized through message-passing interface (MPI) with the techniques of space-decomposition, shift-mode communication, and dynamic load balancing. The result revealed dynamic multi-scale structures characterized by heterogeneity with clustering solids. The solid particle velocity distribution was rather anisotropic, although it was nearly Maxwellian in each direction. The drag forces on the particles were also quite different, and locally structure-dependent to some extent. They were much larger in the dilute phase than those in the center of the dense phase, and become maximum on the phase interface. Besides, the distribution of drag force was somewhat close to the Gaussian function.

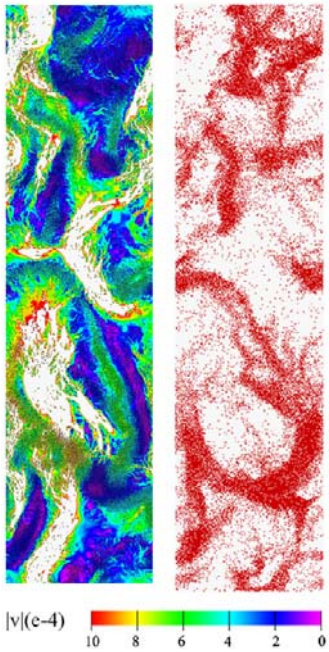

Figure 1: Heterogeneous structure with corresponding velocity field of a gas-solid suspension[27]

With the newly developed general computing technique based on GPU (graphic processing unit), the large computational burden of DNS could be greatly alleviated. Actually, up to 30,000 fluidized solids were further simulated by MaPPM using GPU-based Mole-8.7 HPC (high performance computing) system[27]. The GPU computating in a computer node was realised through CUDA (compute unified device architecture), while the data exchange between different nodes was implemented by MPI technique. Large speedup of nearly 19 folds for one GPU (NVIDIA GT200) over one typical CPU core was achieved. The result reproduced detailed destabilization process of initial uniform suspension and the following formation of solid clusters (Fig. 1). Moreover, the scale-dependence of some important parameters in the suspension with moderate solid/gas density ratio was also revealed. According to the statistical analysis on gas-rich dilute phase and particle-rich dense phase with relatively large solid/gas density ratio (beyond 1000), it was found that the drag coefficient was essentially dependent on the specific cluster configuration.

4 FSI SIMULATION OF OUTFLOW FROM ELASTIC TUBE

Deformation of elastic tube due to the flow of its inner fluids is quite common in both industrial systems and everyday life. To investigate the interaction between weakly compressible fluid and elastic structure, simulation of outflow from elastic tube is carried out with SPH method. As presented in Fig. 2, the particles are initially arranged in a densely packed array of hexagonal lattice inside the whole region. The outer hollow particles represent the elastic microtube, the inner solid bulk represents the fluid, and the solid particles on the rightmost side of the tube are the fixed ends. The flow inside the tube is induced by the control region, where all the particles automatically flow out with the following velocity

$$V_0 = \alpha\sqrt{\rho - \rho_{\text{cri}}} \tag{11}$$

where α is a flow coefficient depending on many factors, including the pressure difference between fluid and outer atmosphere, flow resistance inside the tube, and so forth. Besides, ρ_{cri} is the critical density of fluid, below which the flow would come to an end. When these particles leave the control region, they are immediately eliminated from the simulation. With the quick outflow of inner fluid, the density of fluid would decrease correspondingly, and thus the outflow velocity V_0 would become zero eventually.

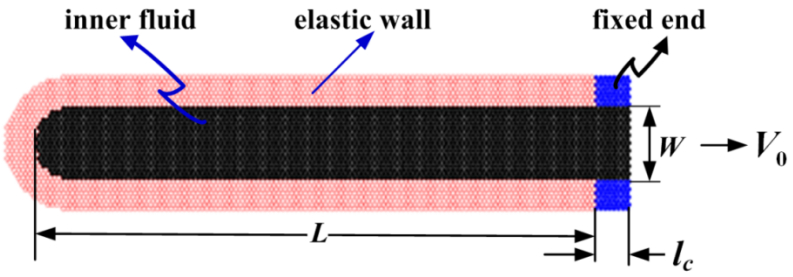

Figure 2: Sketch of elastic tube with initial particle distribution

In our simulation, the length and width of the microtube are L=6.0×10^{-4} m and W=1.0×10^{-3} m. The density of the fluid and solid are ρ_{f}=0.92×10^{3} kg m^{-3} and ρ_{s}=2.76×10^{3} kg m^{-3}, respectively. The length of velocity control region is 4.0×10^{-5} m, the critical density of fluid ρ_{cri} (Eq. 11) is appointed as 0.85ρ_{f}, and the flow coefficient α is 8.615×10^{-5} kg$^{-0.5}$ m$^{2.5}$ s^{-1}. The smoothing length h is 5.333×10^{-5} m, while the numbers of initial fluid particles and solid particles are 35,783 and 2498, respectively. Besides, according to the analysis on dispersion relation of elastic waves[16], the paremeters in the artificial stress (Eqs. 9 and 10) are e=0.3 and q=4. The simulation is switch on at the time t=0.

Fig. 3 displays some typical snapshots during the whole deformation process of elastic tube. With the continuous outflow of fluid in the control region, the inner fluid of the tube is induced to quickly flow out. Since the fluid is weakly compressible, its density gradually becomes smaller, which leads to the reduction of its pressure. The pressure reduction of fluid destroys the initial pressure balance between fluid and tube, resulting in the deformation of the elastic tube. As shown in Figs. 3a-c, with more and more fluid flows out of the tube, the deformation extent of tube increasingly becomes large. Meanwhile, the fluid density and

coreresponding pressure become smaller, and thus the outflow rate of fluid quickly reduces according to Eq. 11. Finally, the fluid flow completely stops due to the zero pressure difference between fluid and outer atmosphere. Fig. 3c is the steady state of this FSI system, where the deformation of tube reaches maximum and fluid density becomes minimum. Note that the deformation of tube in Fig. 3c is so large that the upper and lower sides of this tube nearly connect with each other in their central sections.

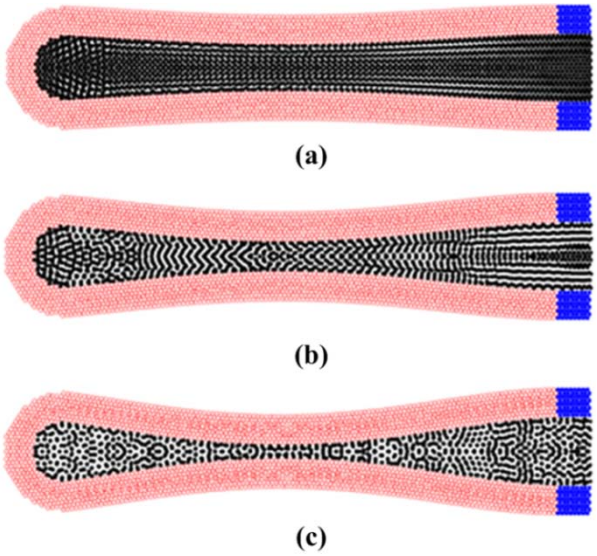

Figure 3: Deformation process of elastic tube due to the outflow of inner fluid: 0.2 s (a), 0.4 s (b), and 1.2 s (c)

4 CONCLUSIONS

As elucidated in the two FSI examples of rigid particles and elastic tube, the FSI simulations with macro-scale particle methods are suitable and also advantageous in providing flow and/or deformation details without complex tracking of interfaces in grid-based numerical techniques. Actually, SPH has been coupled with other particle methods to combine their respective advantages, such as element bending group for modeling flexible fibers[28]. However, the computational cost of macro-scale particle methods is generally rather large (particularly for industrial systems), and thus the further development of efficient algorithm and computational decive would be quite significant in this regard. Besides, the outflow from elastic tube is only preliminarily investigated. Further extension to the liquid-liquid immscible flows (such as water and oil) inside the large-scale complex ealstic and/or rigid structure network would be more meanfuling.

Acknowledgements

This work was supported by the National Key Basic Research Program of China under Grant No. 2015CB251402, the National Natural Science Foundation of China under Grant No. 21206167, 21225628, and 91334204, and the ‘‘Strategic Priority Research Program” of the

Chinese Academy of Sciences under Grant No. XDA07080203. The authors are grateful to Dr. Zhongcun Liu of China Petrochemical Corporation for some helpful discussions.

REFERENCES

[1] Farhat, C., Geuzaine, P., and Brown, G. Application of a three-field nonlinear fluid-structure formulation to the prediction of the aeroelastic parameters of an F-16 fighter. *Comput. Fluids* (2003) **32**:3-29.

[2] Mittal, R., and Iaccarino, G. Immersed boundary methods. *Annu. Rev. Fluid Mech.* (2005) **37**:239-261.

[3] Yu, Z. A DLM/FD method for fluid/flexible-body interactions. *J. Comput. Phys.* (2005) **207**:1-27.

[4] Lucy, L.B. A numerical approach to the testing of the fission hypothesis. *Astron. J.* (1977) **82**:1013-1024.

[5] Gingold, R.A. and Monaghan, J.J. Smoothed particle hydrodynamics: Theory and application to non-spherical stars. *Mon. Not. R. Astron. Soc.* (1977) **181**:375-389.

[6] Ge, W. and Li, J. Simulation of particle-fluid systems with macro-scale pseudo-particle modeling. *Powder Technol.* (2003) **137**:99-108.

[7] Koshizuka, S. and Oka, Y. Moving-particle semi-implicit method for fragmentation of incompressible fluid. *Nucl. Sci. Eng.* (1996) **123**:421-434.

[8] Liu, M. and Liu, G. Smoothed particle hydrodynamics (SPH): An overview and recent developments. *Arch. Comput. Method Eng.* (2010) **17**:25-76.

[9] Zhou, G. and Ge, W. Progress of smoothed particle hydrodynamics in complex flows. *CIESC Journal* (2014) **65**:1145-1161(in Chinese).

[10] Cundall, P.A. and Strack, O.D.L. A discrete numerical model for granular assemblies. *Geotechnique* (1979) **29**:47-65.

[11] Zhu, H.P., Zhou, Z.Y., Yang, R.Y., and Yu, A.B. Discrete particle simulation of particulate systems: Theoretical developments. *Chem. Eng. Sci.* (2007) **62**:3378-3396.

[12] Swegle, J.W., Hicks, D.L., and Attaway, S.W. Smoothed particle hydrodynamics stability analysis. *J. Comput. Phys.* (1995) **116**:123-134.

[13] Dyka, C.T., Randles, P.W., and Ingel, R.P. Stress points for tension instability in SPH. *Int. J. Num. Meth. Engng* (1997) **40**:2325-2341.

[14] Chen, J.K., Beraun, J.E., and Jih, C.J. An improvement for tensile instability in smoothed particle hydrodynamics. *Comput. Mech.* (1999) **23**:279-287.

[15] Monaghan, J.J. SPH without a tensile instability. J Comput Phys (2000) **159**:290-311.

[16] Gray, J.P., Monaghan, J.J., and Swift, R.P. SPH elastic dynamics. *Comput. Methods Appl. Mech. Eng.* (2001) **190**:6641-6662.

[17] Antoci, C., Gallati, M., and Sibilla, S. Numerical simulation of fluid–structure interaction by SPH. *Comput. Struct.* (2007) **85**: 879-890.

[18] Rafiee, A. and Thiagarajan, K.P. An SPH projection method for simulating fluid-hypoelastic structure interaction. *Comput. Methods Appl. Mech. Engrg.* (2009) **198**:2785-2795.

[19] Liu, M., Shao, J., and Li H. Numerical simulation of hydro-elastic problems with smoothed particle hydrodynamics method. *J. Hydrodyn.* (2013) **25**:673-682.

[20] Zhou, G., Ge, W., Li, B., Li, X., and Wang, P., Wang, J., and Li, J. SPH simulation of selective withdrawal from microcavity. *Microfluid. Nanofluid.* (2013) **15**:481-490.

[21] Zhou, G., Chen, Z., Ge, W., and Li, J. SPH simulation of oil displacement in cavity-fracture structures. *Chem. Eng. Sci.* (2010) **65**:3363-3371.

[22] Morris, J.P., Fox, P.J., and Zhu, Y. Modeling low Reynolds number incompressible flows using SPH. *J. Comput. Phys.* (1997) **136**:214-226.

[23] Libersky, L.D., Petschek, A.G., Carney, T.C., Hipp, J.R., and Allahdadi, F.A. High strain Lagrangian hydrodynamics: A three-dimensional SPH code for dynamic material response. *J. Comput. Phys.* (1993) **109**:67-75.

[24] Monaghan, J.J. Simulating free surface flows with SPH. *J. Comput. Phys.* (1994) **110**:399-406.

[25] Potapov, A.V., Hunt, M.L., and Campbell, C.S. Liquid-solid flows using smoothed particle hydrodynamics and the discrete element method. *Powder Technol.* (2001) **116**:204-213.

[26] Ma, J., Ge, W., Wang, X., Wang, J., and Li, J. High-resolution simulation of gas-solid suspension using macro-scale particle methods. *Chem. Eng. Sci.* (2006) **61**:7096-7106.

[27] Xiong, Q., Li, B., Chen, F., Ma, J., Ge, W., and Li, J. Direct numerical simulation of sub-grid structures in gas-solid flow—GPU implementation of macro-scale pseudo-particle modeling. *Chem. Eng. Sci.* (2010) **65**:5356-5365.

[28] Yang, X., Liu, M., and Peng S. Smoothed particle hydrodynamics and element bending group modeling of flexible fibers interacting with viscous fluids. *Phys. Rev. E* (2014) **90**:063011[11 pages].